Mesoscale Wind Farm Placement via Linear Optimization Constrained by Power System and Techno-economics

Ali Erduman, Bahri Uzunoğlu, Bedri Kekezoğlu, and Ali Durusu

***Abstract*—The objective of this study is to develop a wind farm placement and investment methodology based on a linear optimization procedure. This problem has a major significance for the investment success for the projects of renewable energy such as wind power. In this study, a mesoscale approach is adopted whereby the wind farm location is investigated in comparison with a microscale approach where the location of each individual turbine is optimized. Specifical study focuses on the placement of a wind farm by economical optimization constrained by the power system, wind resources, and techno-economics. Linear optimization is introduced in this context at the power system which is constrained by wind farm planning.**

***Index Terms*—Generation expansion, grid integration, mesoscale wind farm, linear optimization, wind power.**

NOMENCLATURE

σ	The first sub-optimization dual factor of wind farm
μ	Limit dual factor of the optimality of wind farm
θ	Busbar degree
Δ	Desired difference
max	Representation of maximum value
min	Representation of minimum value
ε_s	Permitted cut-off value
$BM_{i,j,k,l}$	Unit cost of energy production
BK_l	Number of wind turbines that can be connected to the l^{th} busbar
$BT_{i,j,k,l}$	Turbine technology and busbar
$\boldsymbol{BA}_{j,k}$	Wind turbines with the lowest unit production cost defined for each busbar
$\boldsymbol{BW}_l$	Target height value of the wind power plants to be established before being converted into the matrix form
$\boldsymbol{BR}$	Connection matrix in which the wind power plants can be connected to each busbar according to location technology, and heights within the region
$CF_{i,j,k}$	Capacity factor
$C_{IW,i,j,k}$	Annual investment cost for wind power plants
$C_{OW,i,j,k}$	Annual production cost for wind power plants
$C_{OI,q}$	Annual production cost for installed power plants
$\boldsymbol{dy}$	Vector of load for busbars
F_{mn}	Power flow on transmission line between busbars m and n
GW	Power generated by the planned wind farms
i	Wind farm area index
i_{ter}	Iteration index
j	Wind power plant technology index
k	Available tower height index of selected wind farm technology
l	Busbar index
m, n	Bus number
n_f	Total number of farm areas
n_t	Total number of technologies
n_g	Total number of installed power plants
n_h	Total number of installation heights of wind turbine tower
n_s	Total number of available busbars
g	Power plant index
$\boldsymbol{s}$	Representation of busbar and transmission lines
$\boldsymbol{f}$	Vector of load flow
$ot_{i,j,t}^{i_{ter}}$	Annual maintenance and repair cost
$\boldsymbol{p}$	Matrix of production plants in busbars
$P_g^{\min}$	The lowest generation value of the power plant g
$P_g^{\max}$	The highest generation value of the power plant g

Manuscript received: December 2, 2019; accepted: June 20, 2020. Date of CrossCheck: June 20, 2020. Date of online publication: February 17, 2021.

This work was supported by TUBITAK Scholarship (No. B.14.2.TBT.0.06.01-214-6041) and Yildiz Technical University Scientific Project Coordination Fund (No. 2012-04-02-DOP04).

A. Erduman (correspoding author) is with the Electrical Engineering Department, Hakkari University, Hakkari, 30000 Turkey (e-mail: alierduman@hakkari.edu.tr).

B. Uzunoğlu is with Department of Engineering Sciences, Department of Electrical Engineering, Computational and Data-enabled Science and Engineering in Energy Systems, Uppsala University, 751 21 Uppsala, Sweden, and he is also with Department of Mathematics, Florida State University, Tallahassee, FL 32310, USA, (e-mail: bahri.uzunoglu@angstrom.uu.se).

B. Kekezoğlu and A. Durusu are with the Electrical Engineering Department, Yildiz Technical University, Istanbul, 34220 Turkey (e-mail: bkekez@yildiz.edu.tr; adurusu@yildiz.edu.tr).

DOI: 10.35833/MPCE.2019.000150

P_q	Power generated by installed power plant q
$PL_{mn}^{\max}$	The highest carrying capacity of transmission line
$\boldsymbol{r}$	Vector of the accepted load shedding value for each bus
r_l	Calculated load cut-off value for each bus
X_{mn}	Reactance of the transmission line between the busbars m and n
y	Integer variable of optimization (0-1)
Y	The upper limit of optimization
Z	The lower limit of optimization

I. Introduction

In addition to the rapid depletion of fossil energy sources, the increasing environmental impact of fossil fuels has led to a proactive search for alternative energy sources. Among alternative energy sources, wind energy comes to the forefront owing to its renewable and rapid installation features. The results of Turkish potential wind power are estimated to be 88000 MW [1]. In Turkey, the minimum value of the potential wind power that can be used by the electricity energy network was calculated as 13260 MW [2]. It was found that potential wind power in Turkey has a much higher rate than other European countries. To achieve high shares of variable renewable energies, there is a need to continuously investigate characteristics of local and regional power systems and make necessary transmission upgrades [3].

A probabilistic load flow methodology considering large-scale integration of wind power was proposed in [4]. This methodology can handle significant fluctuations from large-scale integration of wind power. In [5], to examine the potential regional wind energy, it was observed that several data such as the regional wind profile, long-term wind speed distribution, wind distribution according to sectors, height of wind turbine tower to be established, and natural and artificial obstacles in the region should be collectively evaluated. In a similar manner, [6] emphasized the importance of Weibull probability density function (PDF) in the analysis of wind data and demonstrated that the Weibull PDF was the most suitable distribution function for the analysis of the regional wind distribution. The wind atlas analysis and application program (WAsP) was used in [7] to evaluate the measured wind data before estimating the energy produced at different points. With this program, the analysis on potential wind energy was conducted in regions where no measurements were available [8]-[10]. Another important parameter for the accurate evaluation of wind energy is the turbine type used in wind power plants [11], [12]. Among the different types of wind turbines, permanent magnet synchronous generators (PMSGs) and doubly fed induction generators (DFIGs) are the most extensively used [13], [14]. To select the best wind turbine for the region, production technology, production costs, and their effects on power grid connections must be collectively taken into consideration [15]. The approximate weight calculation for a turbine with nominal power, height, and technology was proposed as a function of the weight of the parts [16]. In this regard, [17] conducted an optimization analysis of wind turbines and examined the constraints affecting the turbine structure before proposing solutions for the regional (and country's) target technologies and costs with earthquake constraints. Reference [18] presented a methodology to investigate various effects of power grid integration on the overall operation cost reduction associated with additional wind power in interconnected multi-area power systems. This study concluded that although extra spinning reserves need to be borne by a system proportionate to the output power from wind energy generation, it is always profitable in terms of total operation costs to maximize the output from wind energy generation [18].

In addition to technical constraints [19], [20], wind turbines are also associated with constraints of the installation and production costs [21], [22]. These constraints include the land prices of the area where the wind power plant will be installed, transmission line installation costs, transformer and switchgear system costs, technology-based installation costs, and production costs of other power plant equipment [23].

Supply reliability regulation of Turkey [24] specified the feeder constraints that can be connected to the busbar at a connection point and the connection conditions of wind turbines. These conditions arise in the form of direct constraints in optimal connection studies. As stated above, some or all of these constraints must be considered to determine the network connectivity rates of wind farms. The combined assessment of these constraints underpins the necessity of optimal placement. Reference [25] provided a review of optimization models with integrated generation and transmission expansion planning, which has been tackled by several researchers, revealing the role of transmission networks in the penetration of wind energy systems. The advantages and disadvantages of the methodologies for the optimization of wind energy systems were also given. The Bender decomposition method [26], the Nash equilibrium method [27], and game theory method [28] are some of the leading optimization algorithms that can be used to evaluate different constraints. While the plans for the power system were made using the Bender decomposition method, the objective function was divided into sub-optimization blocks in [29]. The primary purpose function of the economic settlement was divided into sub-purpose functions such as the reliability and optimality. The solving technique was presented under various constraints, such as transmission constraints, nominal power of power plants, and economic load sharing.

Likewise, the placement of microscale and mesoscale wind farms has also been performed by adopting different optimization techniques, as shown in Table I.

To summarize, the list of models and applications in the aforementioned studies used single or multi-objective optimization models. Optimization models for the integration of wind energy systems into the power grid usually aim to capture some of the critical challenges arising from the variable nature of wind energy, multi-objective nature of energy policy formulation, operation issues resulting from the integration of wind energy, and the considerable role of power system characteristics.

TABLE I
MICROSCALE AND MESOSCALE WIND FARM PLACEMENT REPORTED IN LITERATURE

Scale	Flow and wake model	Power system model	Other model used in optimization	Optimization method	Comment or outcome	References
Microscale	Jensen's wake decay model and no flow model	None	None	Mixed integer and quadratic optimization	Basic optimization with no flow model for complex terrain	[30]
Microscale	Jensen's wake decay model and no flow model	None	None	Multi-objective evolutionary algorithm	Multi-objective evolutionary algorithm with a set of Pareto optimal vectors was obtained with objective as maximum output power at minimum wake losses, i.e., at maximum efficiency for several simultaneous wind farm layouts	[31]
Microscale	Jensen's wake decay model and no flow model	None	None	Ant colony algorithm	The algorithm optimization was employed for wind farm layout with wake losses	[32]
Microscale	Jensen's wake decay model and no flow model	None	None	Particle swarm optimization	The problem was formulated by using levelized production cost (LPC) as the objective function	[33]
Microscale	Jensen's wake decay model and no flow model	None	None	Differential evolution	Differential evolution was employed and maximizing the power output of the wind farm was regarded as the optimization objective	[34]
Microscale	Jensen's wake decay model and no flow model	None	None	Genetic and ant colony algorithms	The wake effect, cable parameters, and wind speed series were considered	[35]
Microscale	Jensen's wake decay model and no flow model	None	None	Binary real coded genetic algorithm (BRCGA) and local search (LS) algorithm	Binary part was used to represent the location of turbines, and the real part was used to give the power generated by turbines. By implementing LS technique, optimal solution near the approximated solution was obtained by BRCGA	[36]
Microscale	Jensen's wake decay model calibrated with computational fluid dynamics data	None	None	Sequential convex programming	The locations of a large number of wind turbines were optimized while maximizing the power production	[37]
Mesoscale	None	Mesoscale data model with artificial neural networks	Bathymetry data model with artificial neural networks	Genetic algorithm	Numerical optimization of site selection for offshore wind turbine installation	[38]
Mesoscale	None	Power balance equations	None	Hierarchical Bender decomposition (HBD) technique to solve the proposed probabilistic planning model	Probabilistic generation and transmission expansion planning model based on investment parameters with incentive-based demand response	[39]
Mesoscale	None	Power balance equations	None	Bender decomposition	Generation and transmission expansion planning model based on investment parameters	[40]
Mesoscale	None	Power balance equations	None	Nondominated sorting genetic algorithm-II (NSGA-II), point estimation method (PEM)	Generation and transmission expansion planning model based on investment parameters and wind resource distribution	[41]

This study aims to develop a wind farm placement and investment methodology according to the maximum number of wind farms and minimum installation/production costs under the constraints such as wind potential, power system, and turbine technologies. Within the scope of this study, the original results are listed as follows.

1) The optimization is realized by identifying possible wind areas and shortening the pre-planning time of the wind energy fields.

2) The installation cost components of a power plant are added to the optimization study in detail. Accordingly, the most economical settlement forces of the candidate plants, the connection distances to the energy system, and the costs of these connections are taken into consideration in this study.

3) Economic placement of the system is made by considering not only the regional wind speed, but also its geographical characteristics such as roughness structure and elevation.

4) Using the optimization algorithm, the possibility of selecting the appropriate technology for the region is provided by considering the effects of different technologies on the production cost.

5) When sizing the power plant, the target wind farm is dimensioned for the target region by considering different power options that can be installed in the region.

6) When the energy system constraints are taken into consideration, the questions about how many power plants can be connected to a busbar in economic and technical terms in busbar regions, the total power that can be connected, and the production values upon gaining connection can also be solved with the algorithm.

The remainder paper is organized as follows. In Section II, the theory of the methodological approach is introduced, which is followed by numerical results in Section III and conclusions in Section IV.

II. METHODOLOGY

As shown in Table I, several objective functions can be solved using different methods in the optimization of wind power plants. The studies only considered one or several criteria as the objective function among wind power plant installed power, turbine technology, intra-turbine effects, site impact, impact of network connection criteria and constraints, power plant output power, and plant costs. However, all these criteria need to be considered in real power plant optimization. For example, if the network is not suitable for wind power connection in an area with high potential wind power, it will restrict power plant installation. In this study, a methodology is conducted to consider all of the aforementioned criteria.

The objective of the optimization algorithm is to minimize the production and investment costs of the maximum number of wind farms that can be connected to a region within the power system. The optimization algorithm consists of two linear integer optimization blocks. The first one calculates the maximum number of wind farms that can be connected to a power grid. In the second one, the optimal wind power plant placement that can be connected from the first optimization algorithm is obtained by considering the investment cost, production cost, and reliability.

The minimization of production costs given in the objective function equation is defined as a master problem by integer programming. The sub-programs where production values are controlled, and the feasibility and minimized investment costs are defined as linear programming according to the connection configurations determined by the main program. The Bender decomposition algorithm is used to solve the objective function by dividing it into sub-optimization blocks.

The methodology developed in this study is illustrated in Fig. 1.

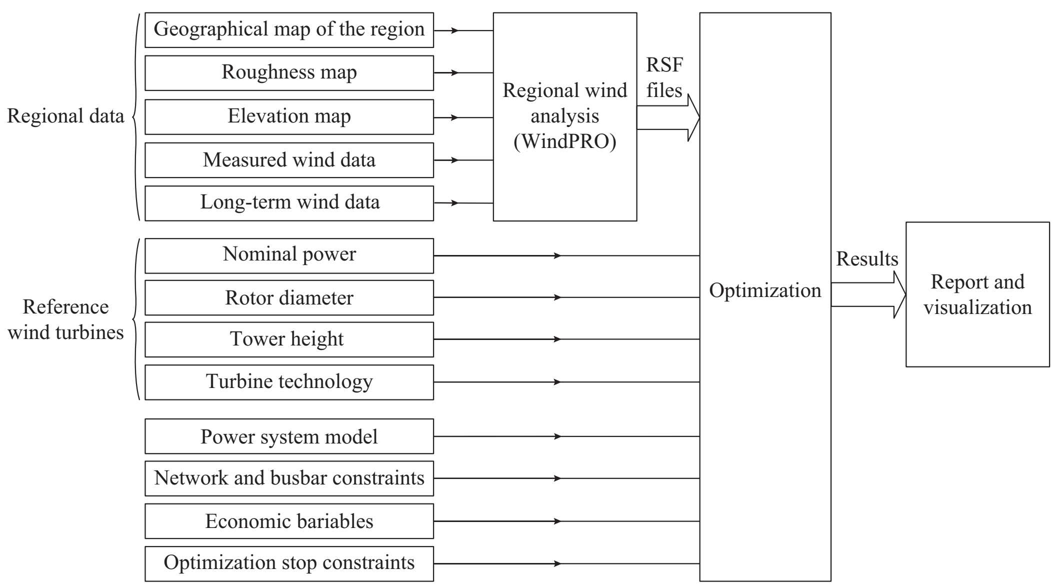

Fig. 1. Flow chart of methodology.

The optimization algorithm given in this study is implemented on an Intel(R) Core(TM) i7-8550U CPU @ 1.80 GHz with 64.0 GB of RAM, and the programs are developed using MATLAB R2014a. Detailed information related to the optimization is provided in the sub-sections.

A. Regional Wind Analysis

To conduct a regional wind analysis, long- and short-term wind speed, wind speed direction data, regional elevation, roughness, and landform information are used. The wind data of Catalca Radar Station from January 1, 2009 to November 1, 2010 are used as reference wind data in the regional wind analysis. This station is at an altitude of 369 m at the coordinates of 41.341185° North latitude and 28.356778° East longitude. For this study, geographic coordinate information is selected on the European side of the city of Istanbul between 41.085° to 41.255° North latitude and 27.929° to 28.784° East longitude. With regard to the scope of this study, surface roughness maps in the data library of the WindPRO/WAsP program are used to calculate natural obstacles without consideration of artificial obstacles [42]. Long-term wind data in the WindPRO/WAsP program library are used to convert the reference wind data into long-term wind data. Within the study scope, digital terrain data based on satellite data of WindPRO online shuttle radar topography mission (SRTM) data set is used and the data are used with 10 m resolution. Moreover, the elevation map is prepared with a working area 7 km longer in all directions to accurately calculate the height data set.

Firstly, the average wind speeds are calculated to generate regional wind speeds according to the reference wind speeds. The mean wind speeds at different altitudes are calculated by subtracting the friction coefficients for each coordinate and the wind distributions in the region according to the reference wind speeds. To calculate point capacity factors, wind speed-power curves of wind turbines with different technologies are converted into mathematical equations by using the curve fitting method with MATLAB. In addition, wind power information, wind speeds, and belly height friction coefficients based on the mathematical model are obtained from the wind turbine database defined in the WindPRO program [43]. In this study, the SIEMENS SWT-3.0-101 and GE-2.85-100 are used as reference wind turbines [44].

B. Maximum Placement Optimization

The input elements of the optimization algorithm are components of the analyzed region (location information and regional geographic map, roughness map, elevation map, long-term wind measurement data, and regional short-term wind measurement data), information of reference wind turbines (nominal power, rotor diameter, tower height, and turbine technologies), power system information (installed plant information, busbar, and transmission lines), network and bus connection restrictions, economic installation and operation data, and optimization constraint information.

A flow diagram of the developed algorithm is illustrated in Fig. 2.

The combination of investment and production costs of the maximum wind farms that can be connected to the system and the mathematical equation for this optimization is provided in (1).

$$\min Y = \sum_{i=1}^{n_f}\sum_{j=1}^{n_s}\sum_{k=1}^{n_t} C_{IW,i,j,k}\, y_{i,j,k} + \sum_{i=1}^{n_f}\sum_{j=1}^{n_s}\sum_{k=1}^{n_t} C_{OW,i,j,k}\cdot GW_{i,j,k} + \sum_{q=1}^{n_g} C_{OI,q} P_q \tag{1}$$

Minimizing the investment cost is stated in (2) as the main problem. The main problem is to establish power plants in the working area with a minimum installation cost. The investment cost is assigned as Z.

$$\min Z \tag{2}$$

The optimization is based on the establishment of wind power plants. Accordingly, the integer variables that each wind farm can take are defined as 0-1 variables. As an additional constraint, (3) is added, after which the main problem is solved.

$$Z \geq \sum_{i=1}^{n_f}\sum_{j=1}^{n_s}\sum_{k=1}^{n_t} C_{IW,i,j,k}\, y_{i,j,k} \tag{3}$$

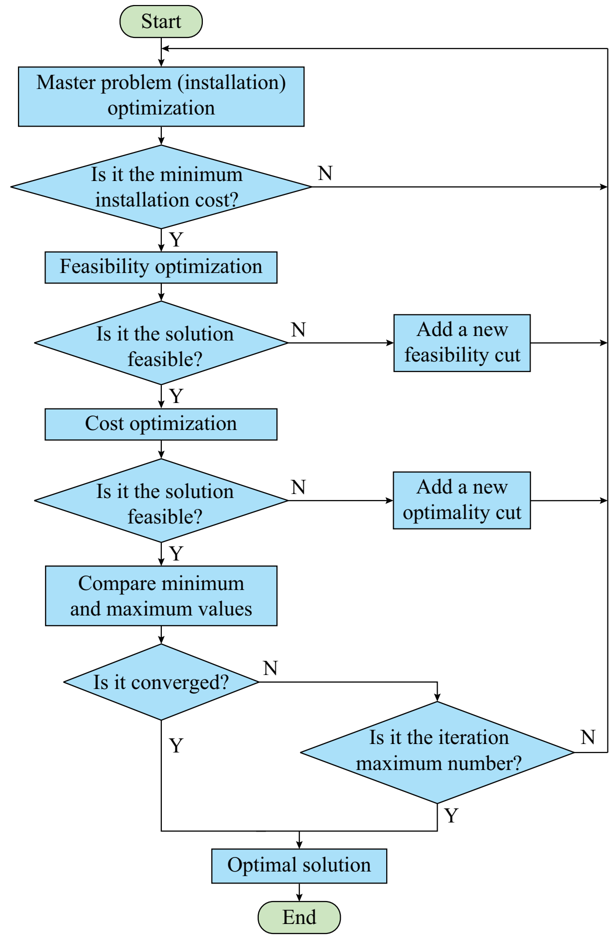

Fig. 2. Flow diagram of economic placement algorithm.

The primary purpose of these sub-problems is to solve the problem related to production costs. However, it is necessary to check whether the system is operating within safe limits before solving this problem. Therefore, the optimization problem can be solved based on the fact that the candidate wind power generation plants selected according to the annual investment cost in the master problem can meet the loads on the system; in other words, the load shedding value is zero.

As a result of these two optimization processes, cost optimization is performed for the case where the limit values are obtained. If the sub-optimization problems cannot be solved under the existing constraints or if there are infinite solutions, the feasibility and optimality multiples will be calculated and added as a constraint to the main problem. According to the reorganized constraints, the main problem is solved again.

As per the second sub-problem, the objective function is to operate the appropriate solutions at optimal production values from the first sub-problem. In this manner, the maximum number of wind farms that can be installed in the power system is determined. The maximum connection number is reduced by one until the optimum connection number is found when the mixed-integer optimization problem could not be solved in the number of connections given at the beginning. The objective function for the maximum number of wind farms that can be connected to the power system (MG), is given in (4).

$$\max MG = \sum_{i=1}^{n_f}\sum_{j=1}^{n_s} GW_{i,j,k}\cdot y_{i,j,k} \tag{4}$$

This step is the production cost optimization. If the optimal value is found as a result of the feasibility optimization, the sub-optimization, where the optimal production value given in (5) is calculated, would be started. The objective of production cost optimization is to minimize the total production cost value. The €/kWh unit obtained from the economic analysis as the production cost value is used by converting €/MWh for production costs. Although the production values of conventional power plants is defined as a parabolic curve under real conditions, it is linearized assuming a constant in this study.

$$\min ot_{i,j,k}^{i_{ter}} = \sum_{i=1}^{n_f}\sum_{j=1}^{n_s}\sum_{k=1}^{n_t} C_{OW,i,j,k}\cdot GW_{i,j,k} + \sum_{q=1}^{n_g} C_{OI,q}P_q \tag{5}$$

The constraints used in the optimization are provided as belows. Accordingly, the maximum number of power plants that can be installed in the system is defined as the sum of the elements whose initial value can be connected to all busbars. In case the optimization at the maximum connection number does not produce appropriate results, the optimization process will be continued by reducing the maximum number until the optimal value is found by using (6).

$$\sum_{i=1}^{n_f}\sum_{j=1}^{n_t}\sum_{k=1}^{n_h} GW_{i,j,k}\cdot y_{i,j,k} \le \sum_{l=1}^{n_s} BK_l \tag{6}$$

The number of wind turbines defined with different technologies and at different heights shall not exceed the maximum connection number defined for the busbar. To achieve the optimization constraint, wind turbines with the lowest unit production cost are defined for each busbar, as illustrated in (7). In the event where the lowest production cost is not available, the element is converted to the matrix form given in (8).

$$f(BM_{i,j,k,l}) = \begin{cases} 1 & BM_{i,j,k,l} = \min\limits_{i=1,2,\ldots,n_f} BM_{i,j,k,l} \\ 0 & \text{otherwise} \end{cases} \tag{7}$$

$$BT_{i,j,k,l} = f(BM_{i,j,k,l}) \tag{8}$$

The matrix $\boldsymbol{BA}_{k,l}$ in (9) is obtained by rearranging $BT_{i,j,k,l}$, which depends on the busbars and turbine technologies.

$$\boldsymbol{BA}_{k,l} = \begin{bmatrix} BT_{1,1,k,l} & BT_{1,2,k,l} & \cdots & BT_{1,n_s,k,l} \\ BT_{2,1,k,l} & BT_{2,2,k,l} & \cdots & BT_{2,n_s,k,l} \\ \vdots & \vdots & & \vdots \\ BT_{n_f,1,k,l} & BT_{n_f,2,k,l} & \cdots & BT_{n_f,n_s,k,l} \end{bmatrix} \tag{9}$$

In (9), the matrices obtained for each technology are recalculated according to the target height value of the wind power plants to be established before being converted into (10).

$$\boldsymbol{BW}_l = \begin{bmatrix} \boldsymbol{BA}_{1,l} & \boldsymbol{BA}_{2,l} & \ldots & \boldsymbol{BA}_{n_t,l} \end{bmatrix} \tag{10}$$

The matrices in (10) are collected by (11) and a connection matrix with n_s rows and n_w columns is obtained for each busbar where the connection and the non-connection values are 1 and 0, respectively.

$$\boldsymbol{BR} = \begin{bmatrix} \boldsymbol{BW}_1 & \boldsymbol{BW}_2 & \ldots & \boldsymbol{BW}_l \end{bmatrix}_{n_s,n_w} \tag{11}$$

The constraint for the connection matrix $\boldsymbol{BR}$ is given in (12).

$$\boldsymbol{BR} \le \begin{bmatrix} BK_1 & BK_2 & \ldots & BK_{n_s} \end{bmatrix}^{\mathrm{T}} \tag{12}$$

The wind farm site is evaluated using multiple technologies, simultaneously. The optimization constraint on the construction of a power plant for the potential farm area is defined in (13).

$$\begin{bmatrix} \sum_{j=1}^{n_t}\sum_{k=1}^{n_h} GW_{1,j,k} & \sum_{j=1}^{n_t}\sum_{k=1}^{n_h} GW_{2,j,k} & \ldots & \sum_{j=1}^{n_t}\sum_{k=1}^{n_h} GW_{n_f,j,k} \end{bmatrix}^{\mathrm{T}} \le \begin{bmatrix} 1 & 1 & \ldots & 1 \end{bmatrix}^{\mathrm{T}} \tag{13}$$

It is checked whether the wind farms are in operation. If the value of the wind farms is enabled, the status is defined as 1, otherwise 0. In (14), the integer changes of the wind farms are defined. Accordingly, it is accepted that wind turbines do not draw power from the power grid.

$$\begin{cases} GW_{i,j,k} \ge 0 \\ GW_{i,j,k} = \mathrm{int}[0,1] \end{cases} \tag{14}$$

The permissible load shedding limits for the reliability requirement considered for the constraint in each busbar are given in (15). If the intention is always meeting all loads in a busbar, the total value of (15) will be assumed to be equal to zero.

$$\sum_{l=1}^{n_s} r_l \le \varepsilon_s \tag{15}$$

The constraint is Kirchhoff's first law, which is shown in (16), and accordingly, the equality of total production in a busbar to total consumption is defined.

$$\boldsymbol{sf} + \boldsymbol{p} + \boldsymbol{r} = \boldsymbol{dy} \tag{16}$$

Kirchhoff's second law, which is considered in the constraint, is given in (17). Meanwhile, the load flow on the power transmission line is defined as the ratio of the phase openings of the busbars, to which the power transmission line is connected.

$$f_{nm} = \frac{\theta_n - \theta_m}{X_{nm}} \tag{17}$$

In the constraint, it is defined that other plants already established in the system should operate between the minimum and maximum production limit values given in (18).

$$P_g^{\min} \le P_g \le P_g^{\max} \quad g = 1, 2, \ldots, n_g \tag{18}$$

According to the constraint, the candidate wind farms in the system should operate between the minimum and maximum limit values given in (19).

$$0 \le GW_{i,j,k} \le GW^{\max}\cdot y_{i,j,k} \tag{19}$$

According to the constraint, the transmission lines in the system must operate between the minimum and maximum limit values given in (20).

$$-PL_{mn}^{\max} \le f_{mn} \le PL_{mn}^{\max} \tag{20}$$

The busbar angles in the system must operate between the minimum and maximum limit values given in (21).

$$\theta_l^{\min} \le \theta_l \le \theta_l^{\max} \tag{21}$$

The maximum number of wind power plants that can be connected is determined by changing the conventional power plant production values as a result of the obtained optimization. Additionally, the maximum number of wind farms determined by the number of wind farm connections are defined as the new bus constraint, which is a subset of the initial bus constraint vector.

New busbar constraints and maximum connectable wind farms are sent as inputs to the Bender separation method. The purpose of the first sub-optimization problem (*ft*) is to ensure that all loads in the working zone operate within the specified load shedding values in (22). As per the scope of this study, it is intended that the needs of load energy can be met and load shedding values ε_l are accepted as zero.

$$\min ft^{i_{ter}} = \sum_{l=1}^{n_s} r_l \le \varepsilon_l \tag{22}$$

The constraint functions of the first sub-optimization problem consist of (15)-(21), which are used to define the DC load flow constraints and the maximum and minimum limits of the variables in the power system. In the first sub-optimization, (21) is rearranged and transformed into (23) and (24).

$$GW_{i,j,k} \le GW^{\max} \cdot y_{i,j,k} \bar{\sigma}_{i,j,k}^{i_{ter}} \tag{23}$$

$$-GW_{i,j,k} \le -GW^{\min} \cdot y_{i,j,k} \underline{\sigma}_{i,j,k}^{i_{ter}} \tag{24}$$

The first dual sub-optimization factors of wind farms, $\bar{\sigma}_{i,j,k}^{i_{ter}}$ and $\underline{\sigma}_{i,j,k}^{i_{ter}}$, are defined as the amounts of production cost reduction in the case of an increase of 1 MW power generation. They are used in the feasibility layer calculation to be added in non-feasible cases, as given in (25). The calculated feasibility level is subsequently added as a constraint to the main optimization problem given in (1).

$$ft^{i_{ter}} + \sum_{i=1}^{n_f}\sum_{j=1}^{n_s}\sum_{k=1}^{n_t}\left(\bar{\sigma}_{i,j,k}^{i_{ter}} GW^{\max} \cdot y_{i,j,k} - \underline{\sigma}_{i,j,k}^{i_{ter}} - GW^{\min} \cdot y_{i,j,k}\right) \le \varepsilon_{i,j,k} \tag{25}$$

If there is no optimal result of the second sub-optimization problem, the calculated optimal coefficient in (28) will be added as a constraint to the main optimization problem given in (1). The equation constraint functions of the second sub-optimization consist of (15)-(21). Equation (19) is rearranged in (26) and (27) to determine the lower and upper limits of wind farms in the constraint equations. The nominal capacity of the wind farms is multiplied by the capacity factor, and the nominal power that the turbine can deliver is determined from (26).

$$GW_{i,j,k} \le GW^{\max} \cdot y_{i,j,k} \cdot CF_{i,j,k} \cdot \bar{\mu}_{i,j,k}^{i_{ter}} \tag{26}$$

$$-GW_{i,j,k} \le -GW^{\min} \cdot y_{i,j,k} \underline{\mu}_{i,j,k}^{i_{ter}} \tag{27}$$

The multipliers $\bar{\mu}_{i,j,k}^{i_{ter}}$ and $\underline{\mu}_{i,j,k}^{i_{ter}}$ represent the dual factors of the optimality of wind farms, and are defined as the amounts of reduction in production costs versus a 1 MW increase in power generation. The constraints of the optimization problem are listed in the following items. The upper optimization limit y is calculated using the formula given in (1), whereas the new lower limit (Z) is defined in (28).

$$Z \ge \sum_{i=1}^{n_f}\sum_{j=1}^{n_t}\sum_{k=1}^{n_h} C_{IW,i,j,k} \cdot y_{i,j,k} + \sum_{j=1}^{n_s}\Big[o\, t_{i,j,k,l}^{i_{ter}} + \left(\mu_{i,j,k}^{i_{ter}} \cdot GW^{\max} \cdot y_{i,j,k} - \underline{\mu}_{i,j,k}^{i_{ter}} \cdot GW^{\min} \cdot y_{i,j,k}\right)\Big] \tag{28}$$

The difference between the lower and upper limits is expressed as optimization termination criteria [45], which is defined in (29). The optimization is terminated if the desired difference Δ is reached or the specified number of iterations is exceeded.

$$\Delta = \frac{2(Y-Z)}{Y+Z} \tag{29}$$

C. Details of Test System

In power system analysis, it is very difficult to analyze the national grid in its entirety. For this reason, selecting the region directly affected by the work and performing the analyses related to the selected region will increase the intelligibility while reducing the calculation time. In this study, the power system section, including the Ikitelli (B1), Buyukcekmece (B2), Catalca (B3), Silivri (B4), Trakya Elektrik (B5), Botas (B6), and Akcansa (B7) busbars in the first transmission system connected to Turkish National Energy Transmission System, is selected as the working area. The coordinates of the selected busbars on the geographical system (35 time zones) are listed in Table II.

TABLE II
BUS LOCATION COORDINATES

Busbar	Busbar name	Easting coordinate (m)	Northing coordinate (m)
B1	Ikitelli	650313	4547902
B2	Buyukcekmece	629085	4543118
B3	Catalca	621401	4554979
B4	Silivri	603448	4550293
B5	Trakya Elektrik	582265	4538903
B6	Botas	581960	4538559
B7	Akcansa	630222	4542388

The lengths of transmission lines between the busbars, the electrical parameters of the transmission lines, the nominal power of the transformers, and the maximum and minimum generation values of the generators were used to model the selected region [46]. The fact that the loads exhibit continuous variability during the study on the first bus was neglected. In the summer of 2012, the maximum consumption occurred on July 27, 2012. The peak production and loads on July 27 at 14:30 were considered constant [46]. In the optimization study, the nominal power of the system components was also taken into consideration.

The single-line diagram of the section within the first transmission system, which is taken as a reference for the modeling of wind energy systems in the Turkey National Electricity Network, is illustrated in Fig. 3. It is notable that busbar B1 is selected as the reference busbar by taking the connection point with the national energy network. The selected busbar is assumed to have infinite power. The rated operation voltage is 154 kV. The information on the loads, generators, transmission lines, and transformers, as shown in Fig. 3, was described in [44]. These values were used for the modeling of power systems in the optimization study.

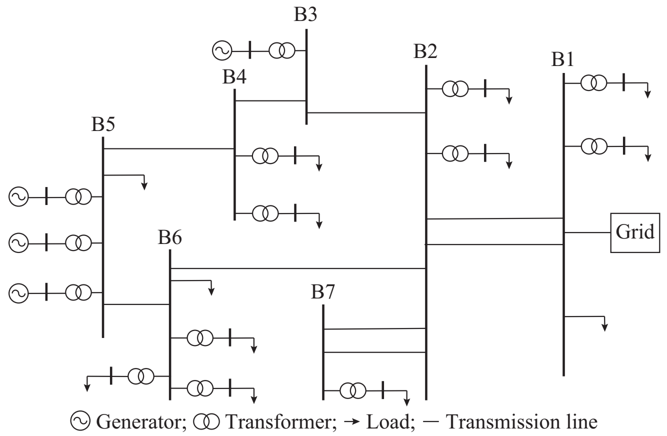

Fig. 3. Single-line diagram of the 7-bus system connected to the first transmission line.

In accordance with the scope of this project, the model belonging to two different wind farm manufacturers, as shown in Table III, and the operation status of these models at installable tower heights were analyzed [43]. The region has been evaluated for 440 potential wind farm areas, two different technologies, and three different heights of each technology. In total, the number of candidate wind farms was calculated as 2460. In the supply reliability regulation of Turkey, the connection number for each busbar in the 154 kV energy transmission systems was defined as 10 [24]. As per this scope, the number of available feeders for each bus is determined by subtracting the total number of the used connections from 10 before being assigned a limitation to the maximum connection optimization, as shown in Table IV. In the optimization, the connection constraint to the busbar is defined as 7. Busbar B1 is determined given that the oscillation busbar and wind farms are not defined at busbar B1.

TABLE III
TECHNICAL FEATURES OF TWO DIFFERENT WIND TURBINES

Manufacturer	Wind turbine type	Power (MW)	Rotor diameters (m)	Rated speed (m/s)
SIEMENS	PMSG	3.00	(74.5, 89.5, 94.0)	16.0
GE	DFIG	2.75	(75.0, 85.0, 98.3)	14.8

TABLE IV
NUMBER OF AVAILABLE FEEDERS FOR BUSBARS

Busbar	Number of available connections
B1	0 (Oscillation busbar)
B2	2
B3	7
B4	6
B5	4
B6	4 (Not selected)
B7	7

III. NUMERICAL RESULT

The lowest cost busbar is selected considering the the coordinate information of the connection point, the transmission line distance to the busbar, the total investment, reduced investment, and unit energy generation values. In the calculations made with a resolution of 200 m × 200 m at a height of 70.0 m, 440 wind areas are found, and each area is calculated based on energy generation, reduced annual energy, and unit energy costs, as depicted in Table V.

TABLE V
TECHNICAL FEATURES OF TWO DIFFERENT WIND TURBINES

Capacity factor	Busbar	Distance to busbar (km)	Total installation cost (M€)	C_{OW} (M€)	*BM* (€/kWh)
0.317	B1	11.82	42.86	3.072	0.022293
	B2	12.26	42.91	3.075	0.022312
	B3	57.73	47.45	3.344	0.024265
	B4	35.35	45.22	3.211	0.023304
	B5	11.87	42.87	3.073	0.022296
	B6	58.10	47.49	3.346	0.024280
	B7	17.94	43.48	3.108	0.022556

In Table V, the lowest unit energy cost of the potential wind farm in the region (the midpoint coordinate of the selected wind farm region is (638800 m, 4550600 m)) is calculated as 0.022293 €/kWh, whereas the candidate wind farm in this coordinate is assigned to B1. With the regulation of regional data, the working area is divided into 440 areas where each 50 MW power plant could be installed. Figure 4 illustrates the distribution of wind power plants in the region when wind turbines are placed in the region separated in accordance with the busbars.

In the maximum connection optimization, the number of initial wind farms that can be connected to all busbars is calculated to be 30. After the maximum connection optimization process, the number is 11 due to power system constraints. The distribution of the 11 wind farms to the busbars is shown in Table VI.

According to the obtained results, the total number of wind farms that can be connected to each bus is arranged as the initial constraint of Bender decomposition optimization.

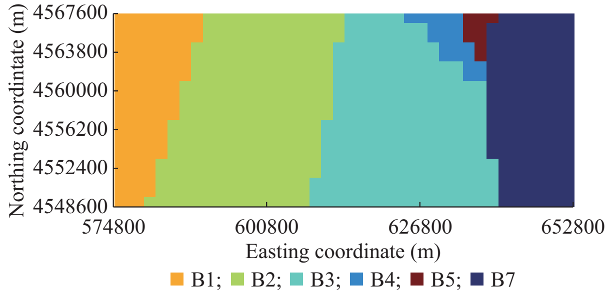

Fig. 4. Distribution of wind farms with a resolution of 200 m × 200 m according to busbars in the test zone.

TABLE VI
BUS CONNECTION CONFIGURATION BASED ON REGULATIONS FOR 7 BUSBARS

Busbar	Number of available connections	Number of optimized connections
B1	0 (Oscillation busbar)	0
B2	2	2
B3	7	1
B4	6	6
B5	4	1
B6	4 (Not selected)	0
B7	7	7

Accordingly, the most economical connection model of the 11 wind farms is calculated in accordance with the configuration, as given in Table VII, using the Bender decomposition optimization. The lower and upper cost values and Δ, which are the stop limits, are given in Table VII.

As a result of the third iteration shown in Fig. 5, the algorithim reaches optimal solution. The sum of investment and production costs decreases from 304.4 to 268.38 M€. The lower limit is calculated as 32.36 M€ in the first iteration. It is calculated as 268.38 M€ in the third iteration, which is the last one with the new optimality constraints added. The convergence time of the algorithm is 10.57 s.

TABLE VII
LOWER AND UPPER COST VALUES AND Δ

Busbar	Δ	Y (M€)	Z (M€)
B1	8.07811×10^{-1}	304	32
B2	1.41220×10^{-2}	268	261
B3	-1.11000×10^{-16}	268	268

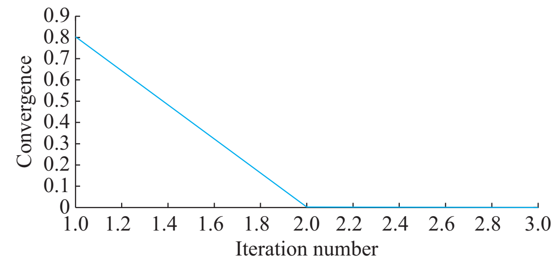

Fig. 5. Convergence of algorithm optimization.

Wind power plant located within the boundaries of B4 is found to be the plant with the highest capacity value in the area. It is also the wind farm with the lowest energy generation cost among the selected turbines, as shown in Table VIII. In terms of the power system, the maximum number of connections is made to B4, followed by B2, B3, B5, and B7. As shown in Table VIII, the SIEMENS-SWT-100 3 MW wind turbine is selected as the most suitable turbine model for this region. According to the cost and turbine power generation values, the wind potential analysis of the region is calculated at the optimum height of 94.0 m, and the PMSG wind turbine is the most suitable. As a result of this optimization process, the distribution of the power plant positions in the working area on the map is shown in Fig. 6. In this regard, the most suitable regional wind power distribution according to the busbars of 200 m×200 m resolution and 94.0 m height is illustrated. Here, each color determines the working area of the busbar, while brown defines the optimal connection points on the area as an optimization result. The busbar connection map shown in Fig. 5 is obtained by placing the geographical location of the power plants on a geographical map. Compared with the existing studies given in Table I, this study differs in terms of the aforementioned criteria, which affect the installation and integration of wind power plants.

TABLE VIII
RESULTS OF PLACEMENT OPTIMIZATION

Easting coordinate (m)	Northing coordinate (m)	Capacity factor	Distance to busbar (km)	Total installation cost (M€)	*BM* (€/kWh)
630800	4550600	0.332	7.68	44.19	0.02203
632800	4550600	0.336	8.35	44.26	0.02178
638800	4566600	0.370	20.92	45.52	0.02055
588800	4556600	0.335	15.95	45.02	0.02217
590800	4558600	0.339	15.13	44.94	0.02191
596800	4548600	0.325	6.86	44.11	0.02236
598800	4548600	0.327	4.95	43.92	0.02216
606800	4548600	0.323	3.76	43.80	0.02237
608800	4548600	0.331	5.61	43.98	0.02199
574800	4556600	0.346	19.21	45.34	0.02171
636800	4548600	0.345	9.05	44.33	0.02134

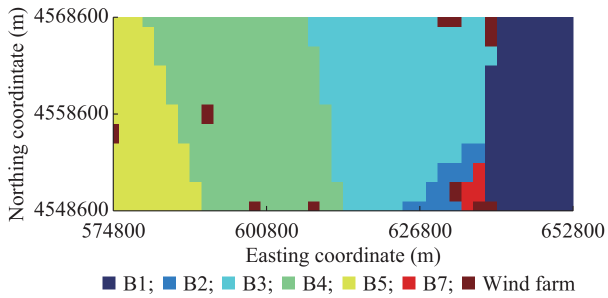

Fig. 6. Representation of busbar-based power plant locations on the map.

IV. Conclusion

By analyzing the potential wind power of a region without consideration of the technical and economic aspects of power system components, it can lead to significant errors in the target planning. As an evaluation result of regional wind data alongside power system components in this study, the endeavor is to obtain more realistic results in determining the connectable regional potential wind power as well as to increase long-term planning accuracy. Through utilizing this developed optimization, the maximum number of wind farms that can be connected to a region as well as the capacity factor of these wind farms and unit energy production costs are obtained.

Thus, in the regional energy planning process, priority comparisons can be calculated as to which power plant can be installed or which regions can receive priority analysis.

Although 50 MW power plants are used as a base, the algorithm, optimization, and functions can be used within different power values.

The effects of different sized wind power plants can be examined. In this manner, the impediments to the use of wind power resources at higher power values can be partially overcome. In this study, the wind turbines with different technologies are considered and compared.

According to both cost and turbine power generation values, the regional potential wind power is analyzed for tower heights of 74.5, 89.5, and 94.0 m, respectively. It is observed that the most suitable height is 94.0 m, and the most suitable technology is the PMSG. When the region is divided into areas with 50 MW power plants, there are 440 potential areas. When the recycling and system connectivity of these candidate plants are technically and economically optimized, it is calculated that 50 MW wind farms in 11 regions can be built and the total annual cost of the wind farm is 268.38 M€. This study specifically focuses on the placement of mesoscale wind farms by economical optimization constrained by power systems, wind resources, and techno-economics. However, the proposed methodology can also be used to optimize large-scale or microscale wind farms. Although wind is used as the energy source in the optimization process prepared in this study, it has an easily adaptable structure for planning other energy sources, especially solar energy.

References

[1] C. İlkiliç, "Wind energy and assessment of wind energy potential in turkey," *Renewable and Sustainable Energy Reviews*, vol. 16, no. 2, pp. 1165-1173, Feb. 2012.

[2] M. Ertürk, "The evaluation of feed-in tariff regulation of Turkey for onshore wind energy based on the economic analysis," *Energy Policy*, vol. 45, pp. 359-367, Jun. 2012.

[3] N. Mararakanye and B. Bekker, "Renewable energy integration impacts within the context of generator type, penetration level and grid characteristics," *Renewable and Sustainable Energy Reviews*, vol. 108, pp. 441-451, Jul. 2019.

[4] X. Deng, P. Zhang, K. Jin *et al.*, "Probabilistic load flow method considering large-scale wind power integration," *Journal of Modern Power Systems and Clean Energy*, vol. 7, no. 4, pp. 813-825, Feb. 2019.

[5] F. A. Jowder, "Wind power analysis and site matching of wind turbine generators in Kingdom of Bahrain," *Applied Energy*, vol. 86, no. 4, pp. 538-545, Apr. 2009.

[6] J. Seguro and T. Lambert, "Modern estimation of the parameters of the Weibull wind speed distribution for wind energy analysis," *Journal of Wind Engineering and Industrial Aerodynamics*, vol. 85, no. 1, pp. 75-84, Mar. 2000.

[7] N. G. Mortensen, D. Heathfield, O. Rathmann *et al.* (2017, Dec.). Wind atlas analysis and application program: WAsP 10 help facility, Technical University of Denmark, Denmark. [Online]. Available: https://core.ac.uk/reader/13802290

[8] D. Mohammed, M. Abdelaziz, A. Sidi *et al.*, "Wind speed data and wind energy potential using Weibull distribution in Zagora, Morocco," *International Journal of Renewable Energy Development*, vol. 8, no. 3, pp. 267-273, Oct. 2019.

[9] Z. Saberi, A. Fudholi, and K. Sopian, "Potential evaluation of wind energy in Kuala Terengganu, Malaysia through Weibull distribution method," *IOP Conference Series: Earth and Environmental Science*, vol. 268, Jul. 2019.

[10] C. F. de Andrade, L. F. dos Santos, M. V. S. Macedo *et al.*, "Four heuristic optimization algorithms applied to wind energy: determination of Weibull curve parameters for three Brazilian sites," *International Journal of Energy and Environmental Engineering*, vol. 10, no. 1, pp. 1-12, Sept. 2019.

[11] T. Ackermann, *Wind Power in Power Systems*, 2nd ed. New York: John Wiley-Sons Inc., 2005.

[12] H. Sun, H. Yang, and X. Gao, "Investigation into spacing restriction and layout optimization of wind farm with multiple types of wind turbines," *Energy*, vol. 168, pp. 637-650, Feb. 2019.

[13] I. Ngamroo, "Review of DFIG wind turbine impact on power system dynamic performances," *IEEE Transactions on Electrical and Electronic Eengineering*, vol. 12, no. 3, pp. 301-311, Feb. 2017.

[14] A. Basit, A. D. Hansen, G. Giannopoulos *et al.*, "Real-time impact of power balancing on power system operation with large scale integration of wind power," *Journal of Modern Power Systems and Clean Energy*, vol. 5, no. 2, pp. 202-210, Nov. 2017.

[15] D. K. Bhutto, J. A. Ansari, S. S. H. Bukhari *et al.*, "Wind energy conversion systems (WECS) generators: a review," in *Proceedings of 2nd International Conference on Computing, Mathematics and Engineering Technologies (iCoMET)*, Sukkur, Pakistan, Mar. 2019, pp. 1-6.

[16] L. Fingersh, M. Hand, and A. Laxson. (2006, Dec.). Wind turbine design cost and scaling model, national renewable energy lab. [Online]. Available: https://www.nrel.gov/docs/fy07osti/40566.pdf

[17] A. Erduman and B. Uzunoglu, "Optimized mesoscale wind farm placement constrained by power system including earthquake damage costs," in *Proceedings of 4th International Conference on System Reliability and Safety*, Rome, Italy, Nov. 2019, pp. 20-22.

[18] J. B. Mogo and I. Kamwa, "Improved deterministic reserve allocation method for multi-area unit scheduling and dispatch under wind uncertainty," *Journal of Modern Power Systems and Clean Energy*, vol. 7, no. 5, pp. 1142-1154, Mar. 2019.

[19] I. Ulku and C. Alabas-Uslu, "A new mathematical programming approach to wind farm layout problem under multiple wake effects," *Renewable Energy*, vol. 136, pp. 1190-1201, Jun. 2019.

[20] M. Shafiee and J. D. Sørensen, "Maintenance optimization and inspection planning of wind energy assets: models, methods and strategies," *Reliability Engineering & System Safety*, vol. 192, p. 105993, Dec. 2019.

[21] J. Bosch, I. Staffell, and A. D. Hawkes, "Global levelised cost of electricity from offshore wind," *Energy*, vol. 189, Dec. 2019.

[22] C. Maienza, A. M. Avossa, F. Ricciardelli *et al.*, "A comparative analysis of construction costs of onshore and shallow-and deep-water offshore wind farms," *Lecture Notes in Civil Engineering, Springer*, vol. 27, pp. 440-453, Mar. 2019.

[23] S. Nikkhah and A. Rabiee, "Optimal wind power generation investment, considering voltage stability of power systems," *Renewable en-*

ergy, vol. 115, pp. 308-325, Jan. 2018.

[24] Turkish Electricity Regulation. (2014, Oct.). The transmission system supply reliability and quality regulation. [Online]. Available: https://www. emo. org. tr/ekler/aadca7bd86c4743_ek. pdf? tipi=38&turu=X&sube=0

[25] A. S. Dagoumas and N. E. Koltsaklis, "Review of models for integrating renewable energy in the generation expansion planning," *Applied Energy*, vol. 242, pp. 1573-1587, May 2019.

[26] M. Shahidehopour and Y. Fu, "Benders decomposition: applying benders decomposition to power systems," *IEEE Power and Energy Magazine*, vol. 3, pp. 20-21, Mar. 2005.

[27] J. Nemcova, M. Petreczky, and J. H. van Schuppen, "Realization theory of Nash systems," *SIAM Journal on Control and Optimization*, vol. 51, no. 5, pp. 3386-3414, May 2013.

[28] M. Shahidehpour, H. Yamin, and Z. Li, *Market Operations in Electric Power Systems: Forecasting, Scheduling, and Risk Management*, New York: John Wiley-Sons Inc., 2002, pp. 1-18.

[29] F. Wu, Z. Yen, Y. Hou *et al*., "Applications of AI techniques to generation planning and investment," in *Proceedings of IEEE PES General Meeting*, Denver, USA, Jun. 2004, pp. 936-940.

[30] S. D. O. Turner, D. A. Romero, P. Y. Zhang *et al*., "A new mathematical programming approach to optimize wind farm layouts," *Renewable Energy*, vol. 63, pp. 674-680, Mar. 2014.

[31] P. P. Biswas, P. N. Suganthan, and G. A. J. Amaratunga, "Decomposition based multi-objective evolutionary algorithm for windfarm layout optimization," *Renewable Energy*, vol. 115, pp. 326-337, Jan. 2018.

[32] S. U. Seçkiner, "Design of wind farm layout using ant colony algorithm," *Renewable Energy*, vol. 44, pp. 53-62, Aug. 2012.

[33] P. Hou, S. Member, W. Hu *et al.*, "Optimized placement of wind turbines in large-scale offshore wind farm using particle swarm optimization algorithm," *IEEE Transactions on Sustainable Energy*, vol. 6, no. 4, pp. 1272-1282, Jun. 2015.

[34] Y. Wang, H. Liu, H. Long *et al.*, "Differential evolution with a new encoding mechanism for optimizing wind farm layout," *IEEE Transactions on Industrial Informatics*, vol. 14, no. 3, pp. 1040-1054, Sept. 2018.

[35] Y. K. Wu, C. Y. Lee, C. R. Chen *et al*., "Optimization of the wind turbine layout and transmission system planning for a large-scale offshore wind farm by AI technology," *IEEE Transactions on Industry Applications*, vol. 50, no. 3, pp. 2071-2080, May 2014.

[36] A. M. Abdelsalam and M. A. El-shorbagy, "Optimization of wind turbines siting in a wind farm using genetic algorithm based local search," *Renewable Energy*, vol. 123, pp. 748-755, Aug. 2018.

[37] J. Park and K. H. Law, "Layout optimization for maximizing wind farm power production using sequential convex programming," *Applied Energy*, vol. 151, pp. 320-334, Aug. 2015.

[38] K. H. Lee, S. O. Jun, K. H. Pak *et al.*, "Numerical optimization of site selection for offshore wind turbine installation using genetic algorithm," *Current Applied Physics*, vol. 10, no. 2, pp. 302-306, Mar. 2010.

[39] C. Li, Z. Y. Dong, G. Chen *et al.*, "Flexible transmission expansion planning associated with large-scale wind farms integration considering demand response," *IET Generation, Transmission & Distribution*, vol. 9, no. 15, pp. 2276-2283, Nov. 2015.

[40] Y. Gu, J. D. McCalley, and M. Ni, "Coordinating large-scale wind integration and transmission planning," *IEEE Transactions on Sustainable Energy*, vol. 3, no. 4, pp. 652-659, Oct. 2012.

[41] M. Moeini-Aghtaie, A. Abbaspour, and M. Fotuhi-Firuzabad, "Incorporating large-scale distant wind farms in probabilistic transmission expansion planning – Part II: case studies," *IEEE Transactions on Power Systems*, vol. 27, no. 3, pp. 1594-1601, Aug. 2012.

[42] K. Murthy and O. Rahi, "A comprehensive review of wind resource assessment," *Renewable and Sustainable Energy Reviews*, vol. 72, pp. 1320-1342, May 2017.

[43] P. Nielsen. (2019, Dec.). Windpro 2.7 user guide, 3rd ed. [Online]. Available: http://www. emd. dk/files/windpro/manuals/for_print/MANUAL_2.7.pdf

[44] A. Erduman, "Determination of optimum wind energy integration potential in National Energy Grid" Ph. D. dissertation, Department of Electrical Engineering, Yildiz Technical University, Istanbul, Turkey, 2015.

[45] M. Shahidehpour and Y. Fu, "Benders decomposition in restructured power systems," *IEEE Power and Energy Magazine*, vol. 3, no. 2, pp. 20-21, Mar. 2005.

[46] A. Erduman, B. Uzunoglu, and A. Durusu, "A new pre-processing for assessing connection areas for busbars of wind power plants using meteorological, financial and electrical grid data," *Gazi University Science Journal: PART C Design and Technology*, vol. 7, pp. 676-687, Sept. 2019.

Ali Erduman received the M.Sc. degree from Abant Izzet Baysal University, Bolu, Turkey, in 2005, and the Ph.D. degree at Yildiz Technical University, Istanbul, Turkey, in 2015. He is an Assistant Professor in the Department of Electrical-Electronics Engineering, Hakkari University, Hakkari, Turkey. His research interests include optimal operation and reliability evaluation of integrated energy system.

Bahri Uzunoğlu received the Ph. D. degree in computational engineering from Southampton University, Southampton, U.K., in 2001. He is currently an Associated Professor in engineering sciences with specialization in computational science of electricity with Uppsala University Electricity Division, Uppsala, Sweden. His industry and academic experience include computational engineering and science applied to renewable energy problems.

Bedri Kekzoğlu received the M. Sc. and Ph. D. degrees at Yildiz Technical University, Istanbul, Turkey, in 2007 and 2013, respectively. He is an Assistant Professor in the Department of Electrical Engineering, Yildiz Technical University. His research interests include optimal operation and reliability evaluation of integrated energy system and renewable energy.

Ali Durusu received the M.Sc. and Ph.D. degrees at Yildiz Technical University, Istanbul, Turkey, in 2011 and 2016, respectively. He is working as a Research Assistant in the Department of Electrical Engineering, Yildiz Technical University. His research interests include power system modelling, control, and renewable energy.